Noname manuscript No.
(will be inserted by the editor)

Design and Simulation of a Silicon Mach–Zehnder Interferometer

Deepanshu Yadav

the date of receipt and acceptance should be inserted later

Abstract This report presents the design and simulation of a silicon-on-insulator Mach–Zehnder Interferometer (MZI) using strip waveguides. Eigenmode simulations are performed to extract the effective and group indices of the waveguide as a function of wavelength. A compact polynomial model is developed for use in system-level simulations. The interferometer transfer function is derived analytically and verified using Lumerical INTERCONNECT simulations. The free spectral range (FSR) of unbalanced MZIs with different path length differences is analyzed, providing a method for extracting the waveguide group index from experimental measurements.

1 Introduction

Silicon photonics enables large-scale integration of optical components using CMOS-compatible fabrication processes, offering compact footprint, high refractive index contrast, and low-cost manufacturing [**?**]. Among the fundamental building blocks of silicon photonic integrated circuits, the Mach–Zehnder Interferometer (MZI) is widely used for optical modulation, filtering, switching, and sensing applications.

The objective of this course project is to design and simulate a silicon-based MZI, develop an accurate waveguide compact model, and establish a framework for extracting the waveguide group index from measured transmission spectra. The device is modeled using Lumerical MODE Solutions and INTERCONNECT, while the physical layout is implemented using KLayout.

THz-Photonics Group, Technische Universität Braunschweig, Schleinitzstrasse 22, 38106, Braunschweig, Germany
Affiliation not available

2 Theory

Firstly, let's consider a y-branch splitter. We begin with an input intensity, I_i, with electric field, E_i. The light is split equally into two branches. Each output has intensity $I_1 = I_2 = I_i/2$, and electric field, $E_1 = E_2 = E_i/\sqrt{2}$. For the combiner, light input in one branch is split equally between the fundamental mode of the waveguide and the higher order modes (or radiation modes). Thus the electric field at the combiner port output will be $E_{o1} = E_1/\sqrt{2}$ or $E_{o2} = E_2/\sqrt{2}$. With two inputs, the output field is a vector summation of the input fields, divided by $\sqrt{2}$, that is

$$E_o = \frac{E_1 + E_2}{\sqrt{2}}.$$

For plane wave, the electric field $E = E_0 e^{i(\omega t - \beta z)}$ and propagation constant $\beta = \frac{2\pi n}{\lambda}$, where n is the index of refraction. For the lossless case,

$$E_{o1} = E_1 e^{-i\beta L_1} = \frac{E_i}{\sqrt{2}} e^{-i\beta L_1} \tag{1}$$

$$E_{o2} = E_2 e^{-i\beta L_2} = \frac{E_i}{\sqrt{2}} e^{-i\beta L_2} \tag{2}$$

Hence the output of the y-branch is

$$E_o = \frac{E_{o1} + E_{o2}}{\sqrt{2}} = \frac{E_i}{2}\left(e^{-i\beta L_1} + e^{-i\beta L_2}\right) \tag{3}$$

And the intensity is

$$I_o = \frac{I_i}{4}\left|e^{-i\beta L_1} + e^{-i\beta L_2}\right|^2 = \frac{I_i}{2}\left[1 + \cos(\beta \Delta L)\right] \tag{4}$$

2.1 Waveguide Dispersion Model

The propagation constant of a guided mode is given by

$$\beta(\lambda) = \frac{2\pi n_{\text{eff}}(\lambda)}{\lambda}, \tag{5}$$

where n_{eff} is the effective index of the waveguide mode.

The group index is defined as

$$n_g(\lambda) = n_{\text{eff}}(\lambda) - \lambda \frac{dn_{\text{eff}}(\lambda)}{d\lambda}. \tag{6}$$

2.2 Mach–Zehnder Interferometer Transfer Function

An unbalanced MZI introduces a path length difference ΔL between its two arms. Assuming equal power splitting and negligible loss, the normalized transmission is

$$T(\lambda) = \frac{1}{2}\left[1 + \cos\left(\beta(\lambda)\Delta L\right)\right]. \tag{7}$$

3 Modelling and Simulation

3.1 Waveguide Geometry and Mode Profile

The device is implemented on a silicon-on-insulator platform with a strip waveguide geometry. The waveguide height is 220 nm and the width is 500 nm. The fundamental quasi-TE polarization is used throughout this work due to its strong optical confinement and reduced bending loss. Apart from this the investigation is also made for TM polarisation for the same strip waveguides.

Figure **??** shows the simulated electric field intensity profile of the fundamental TE mode and TM mode obtained using Lumerical MODE Solutions.

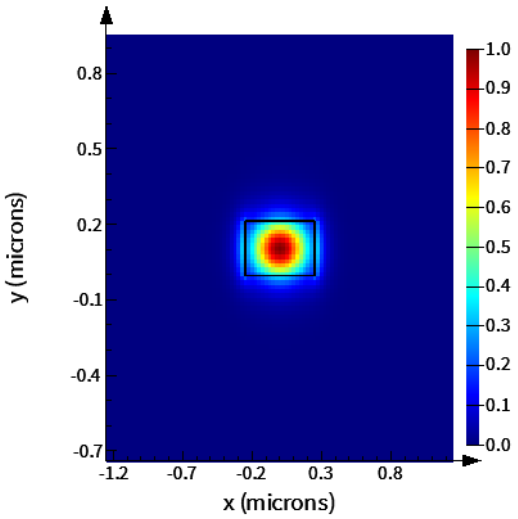

(a) Fundamental quasi-TE mode

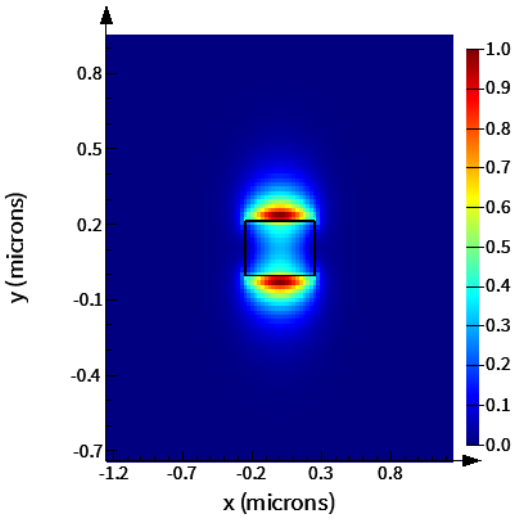

(b) Fundamental quasi-TM mode

Fig. 1: Simulated electric field intensity profiles of the fundamental modes for the strip waveguide.

3.2 Effective and Group Index

The effective index is extracted over the wavelength range of interest. The group index is computed numerically using the dispersion relation.

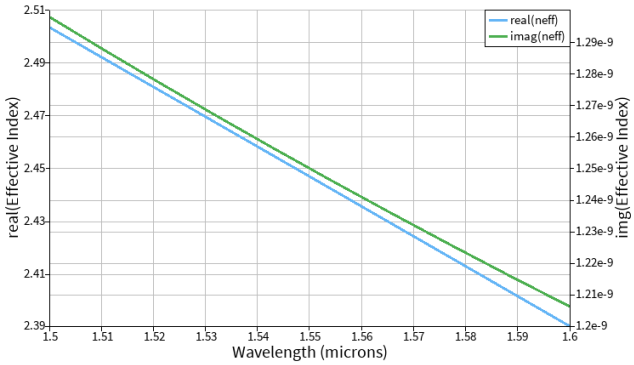

(a)

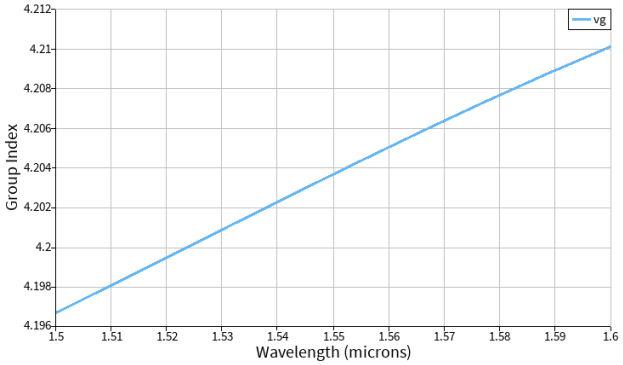

(b)

Fig. 2: (a) Effective index and (b) group index versus wavelength for the TE mode.

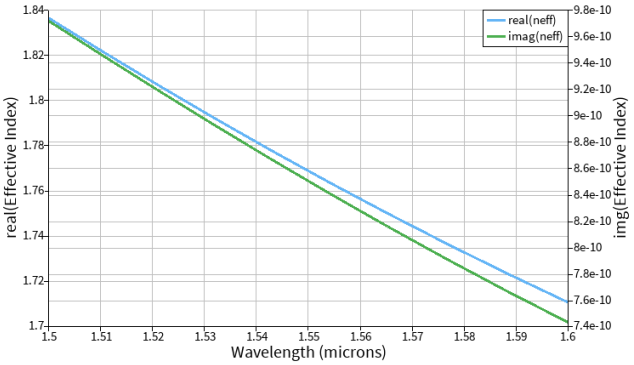

(a)

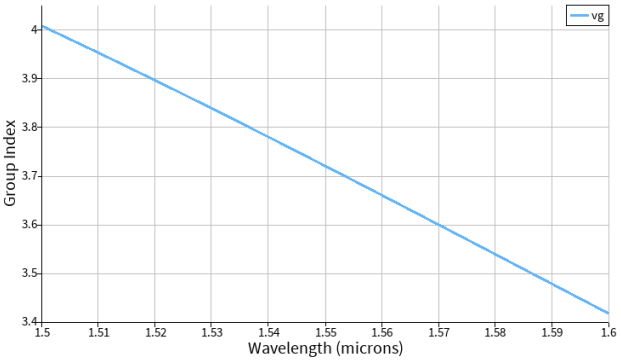

(b)

Fig. 3: (a) Effective index and (b) group index versus wavelength for the TM mode.

3.3 Compact Waveguide Model

The effective index is approximated using a second-order polynomial expansion around $\lambda_0 = 1.55$ μm:

$$n_{\text{eff}}(\lambda) = a_0 + a_1(\lambda - \lambda_0) + a_2(\lambda - \lambda_0)^2. \tag{8}$$

The fitted coefficients are obtained from numerical simulation and used in system-level modeling.
Using matlab, the compact model of the waveguide can be calculated, which gives the equation,

$$n_{\text{eff}}(\lambda) = 2.44682 - 1.13339(\lambda - \lambda_0) - 0.0439366(\lambda - \lambda_0)^2. \tag{9}$$

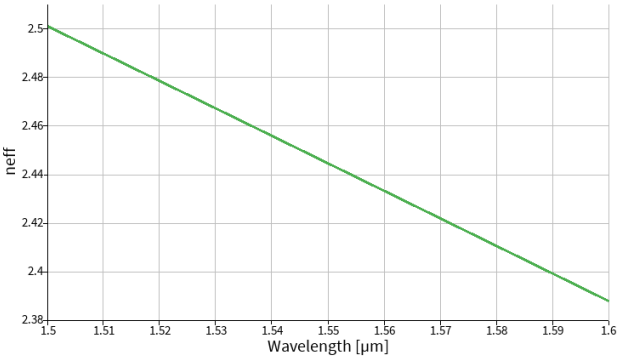

Fig. 5: Compact model of the TE mode, in terms of the effective index. Markers indicate MODE data, and solid lines correspond to a Taylor-series approximation. $n_{\text{eff}}(\lambda) = 2.44682 - 1.13339(\lambda - \lambda_0) - 0.0439366(\lambda - \lambda_0)^2$.

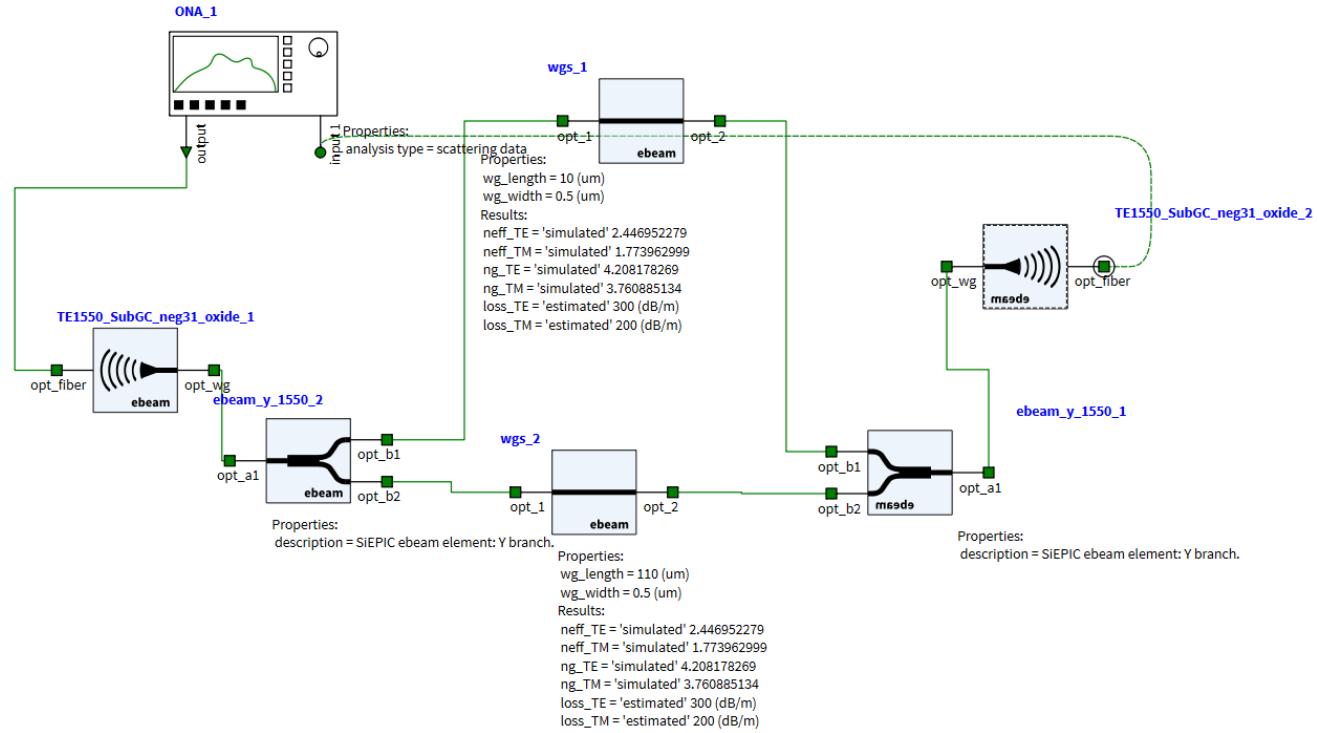

Fig. 4: MZI model implemented in the INTERCONNECT software. ONA: optical network analyzer.

3.4 MZI Parameter Variations

Several MZIs with different path length differences ΔL are designed to study the dependence of free spectral range on geometry.

Table 1: MZI design parameters and expected performance

ΔL (μm)	Expected FSR (nm)	Cell label
0	0	TE-MZI1
30	17.53	TE-MZI2
60	9.37	TE-MZI3
120	4.80971	TE-MZI4
505	1.0832	TE-MZI5
50	12.38	TM-MZI1
100	6.2	TM-MZI2
150	2.798	TM-MZI3

3.5 Transmission Spectrum

System-level simulations are performed using Lumerical INTERCONNECT. Figure 10 shows the simulated transmission spectrum of an unbalanced MZI.

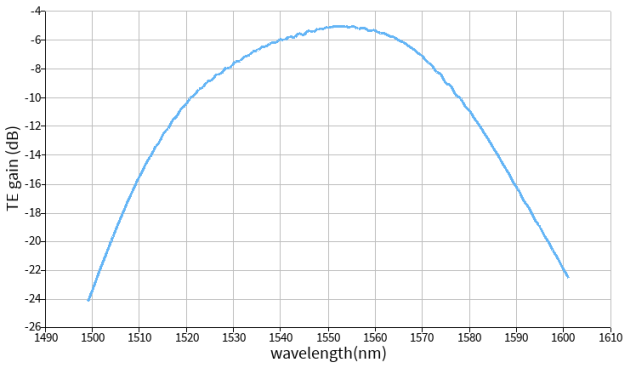

(a)

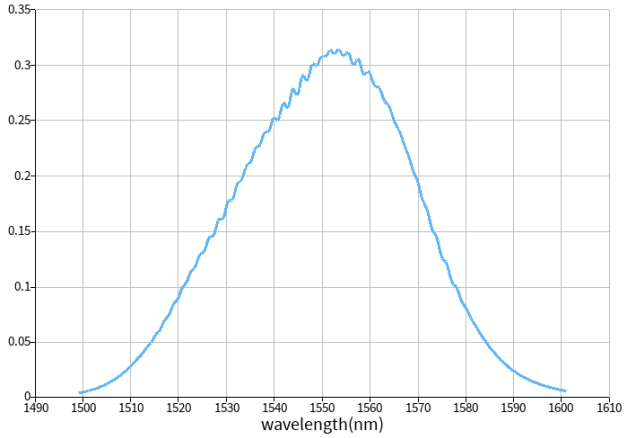

(b)

Fig. 6: (a)Transfer function and (b) Transmission spectrum of MZIs for TE polarisation with length mismatches equal to 0 µm.

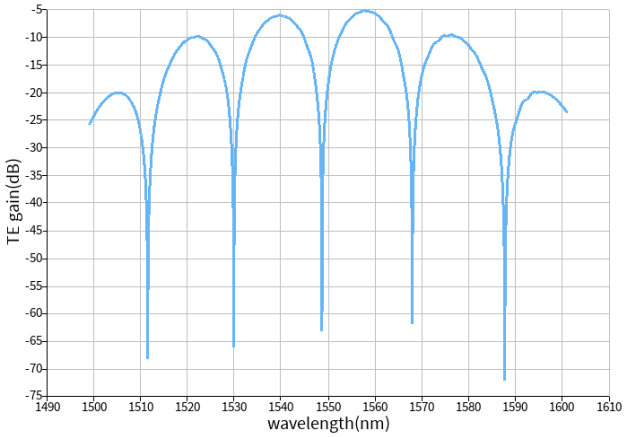

(a)

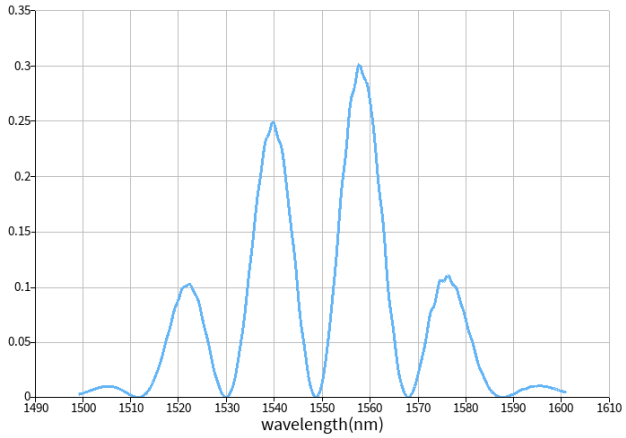

(b)

Fig. 7: (a)Transfer function and (b) Transmission spectrum of MZIs for TE polarisation with length mismatches equal to 30 µm.

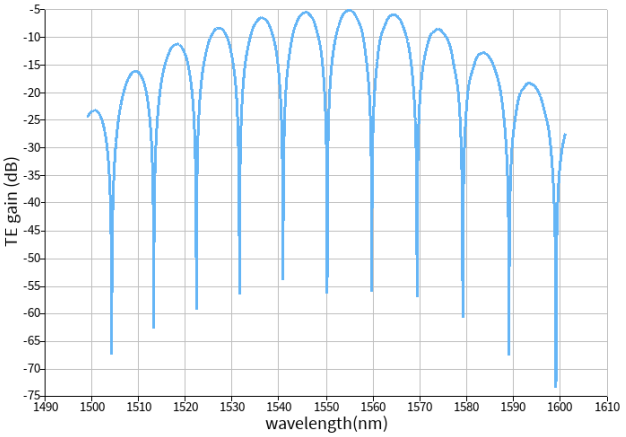

(a)

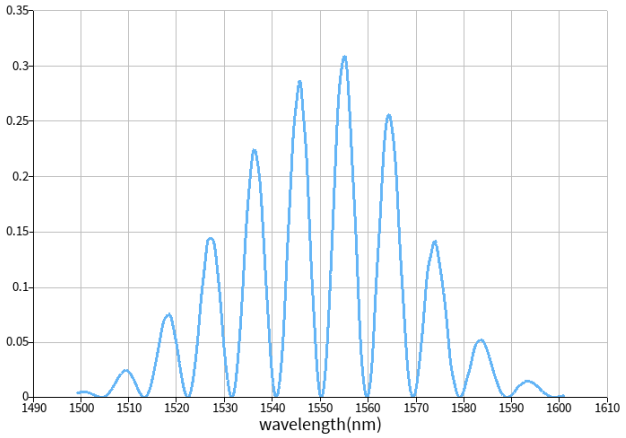

(b)

Fig. 8: (a)Transfer function and (b) Transmission spectrum of MZIs for TE polarisation with length mismatches equal to 60 µm.

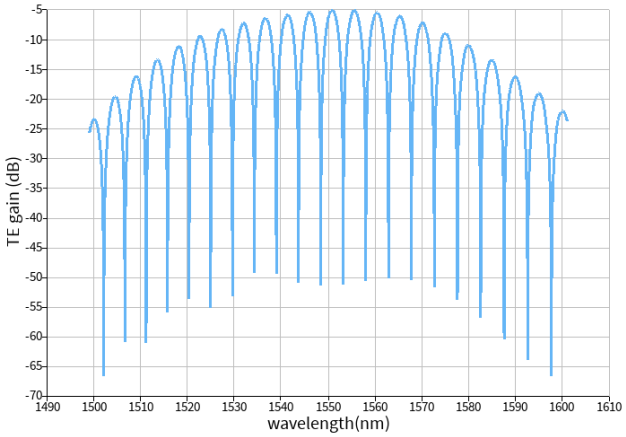

(a)

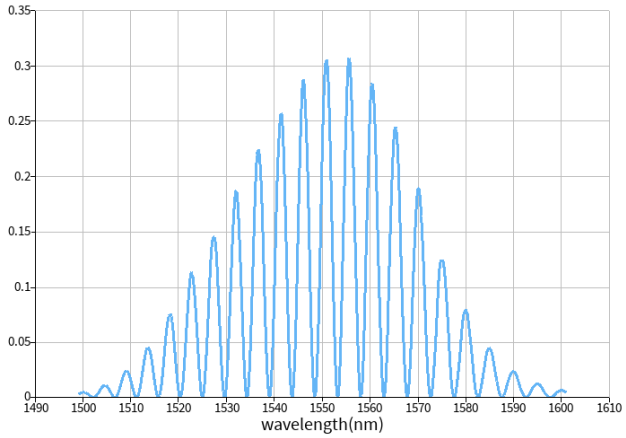

(b)

Fig. 9: (a)Transfer function and (b) Transmission spectrum of MZIs for TE polarisation with length mismatches equal to 120 µm.

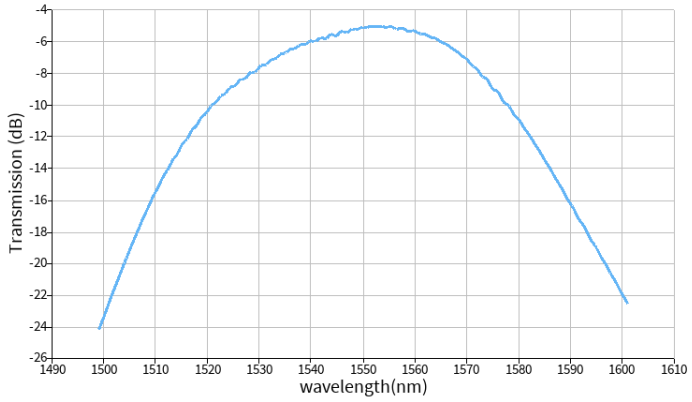

Fig. 10: Simulated transmission spectrum of a Mach–Zehnder Interferometer.

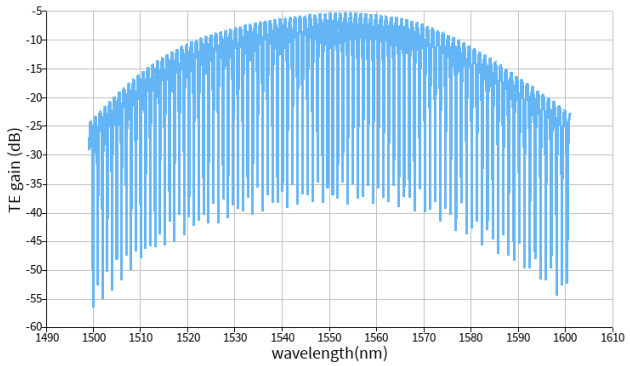

(a)

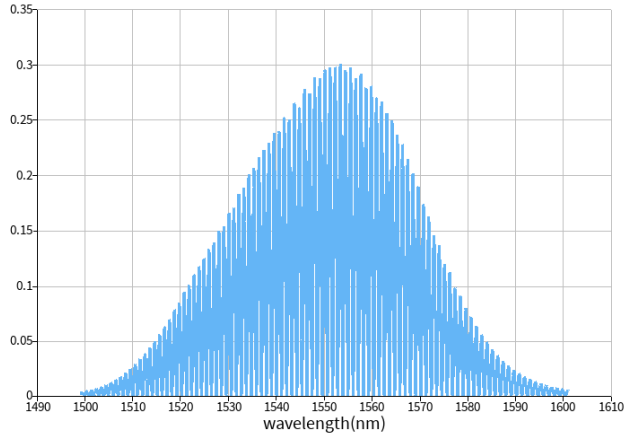

(b)

Fig. 11: (a)Transfer function and (b) Transmission spectrum of MZIs for TE polarisation with length mismatches equal to 505 µm.

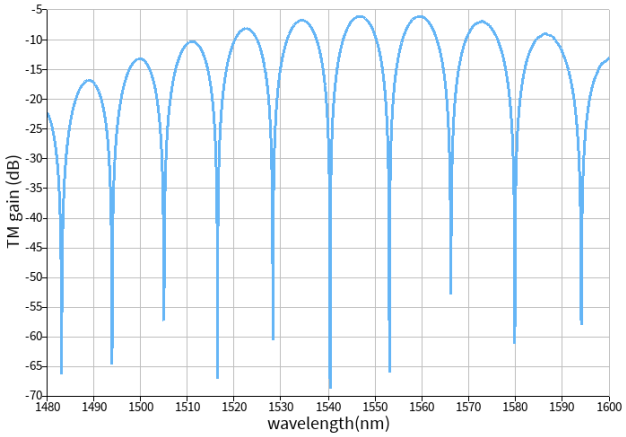

(a)

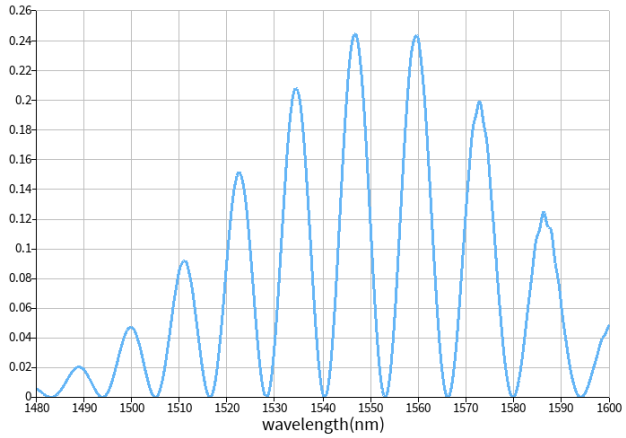

(b)

Fig. 12: (a)Transfer function and (b) Transmission spectrum of MZIs for TM polarisation with length mismatches equal to 50 µm.

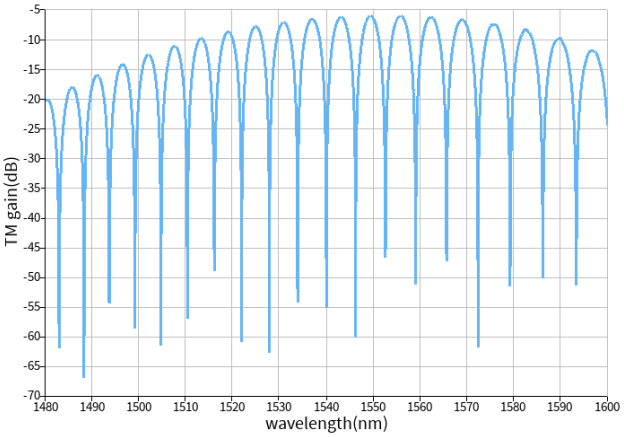

(a)

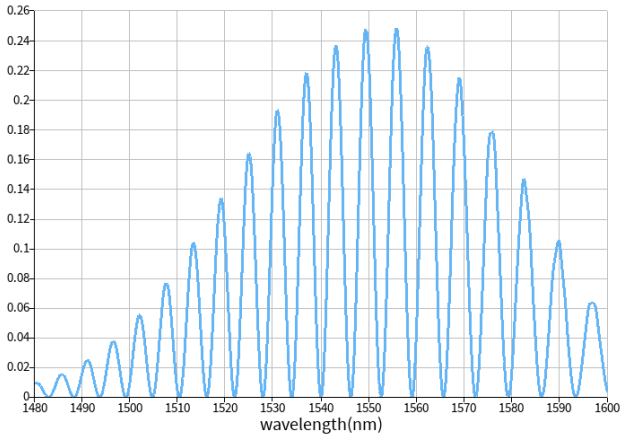

(b)

Fig. 13: (a)Transfer function and (b) Transmission spectrum of MZIs for TM polarisation with length mismatches equal to 100 µm.

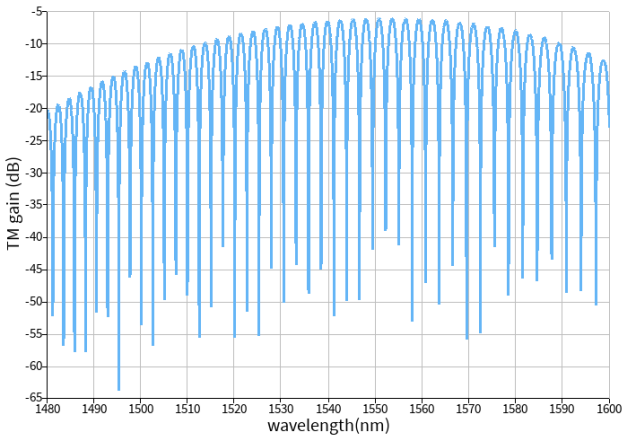

(a)

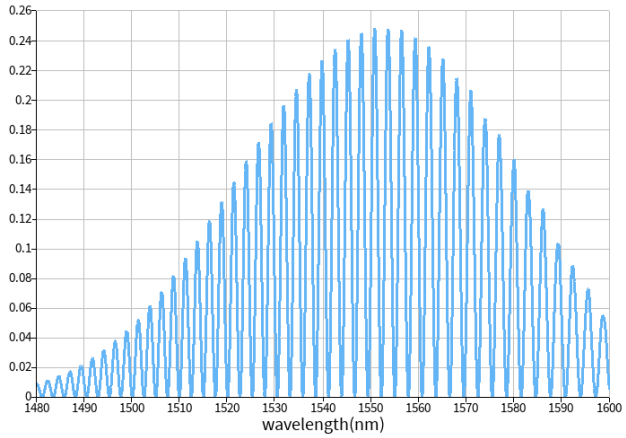

(b)

Fig. 14: (a)Transfer function and (b) Transmission spectrum of MZIs for TM polarisation with length mismatches equal to 150 µm.

4 Layout

The physical layout of the Mach–Zehnder Interferometer (MZI) is designed using KLayout in conjunction with the SiEPIC-EBeam-PDK. In this I have designed the 8 MZI as shown in Figure. 15 with there de-embedding structures working as caliberation test. In MZI 5 of them named "TE-MZI1","TE-MZI2","TE-MZI3","TE-MZI4","TE-MZI5" are TE polarised with their de-embedding structure named "TE-Cali". The other 3 MZI named "TM-MZI1","TM-MZI2","TM-MZI3" are TM polarised with their de-embedding structure named "TM-Cali". These MZI have variation of path difference listed in Table 1 with their corresponding FSR values.

5 Fabrication

One chip was fabricated in this course. Either report on one dataset, or on both. Rest will be updated in future after chip fabrication and getting experimental data for analysis.

5.1 Washington Nanofabrication Facility (WNF) silicon photonics process:

The devices were fabricated using 100 keV Electron Beam Lithography [[2]]. The fabrication used silicon-on-insulator wafer with 220 nm thick silicon on 3 µm thick silicon dioxide. The substrates were 25 mm squares diced from 150 mm wafers. After a solvent rinse and hot-plate dehydration bake, hydrogen silsesquioxane resist (HSQ, Dow-Corning XP-1541-006) was spin-coated at 4000 rpm, then hotplate baked at 80 °C for 4 minutes. Electron beam lithography was performed using a JEOL JBX-6300FS system operated at 100 keV energy, 8 nA beam current, and 500 µm exposure field size. The machine grid used for shape placement was 1 nm, while the beam stepping grid, the spacing between dwell points during the shape writing, was 6 nm. An exposure dose of 2800 µC/cm2 was used. The resist was developed by immersion in 25% tetramethylammonium hydroxide for 4 minutes, followed by a flowing deionized water rinse for 60 s, an isopropanol rinse for 10 s, and then blown dry with nitrogen. The silicon was removed from unexposed areas using inductively coupled plasma etching in an Oxford Plasmalab System 100, with a chlorine gas flow of 20 sccm, pressure of 12 mT, ICP power of 800 W, bias power of 40 W, and a platen temperature of 20 °C, resulting in a bias voltage of 185 V. During etching, chips were mounted on a 100 mm si-

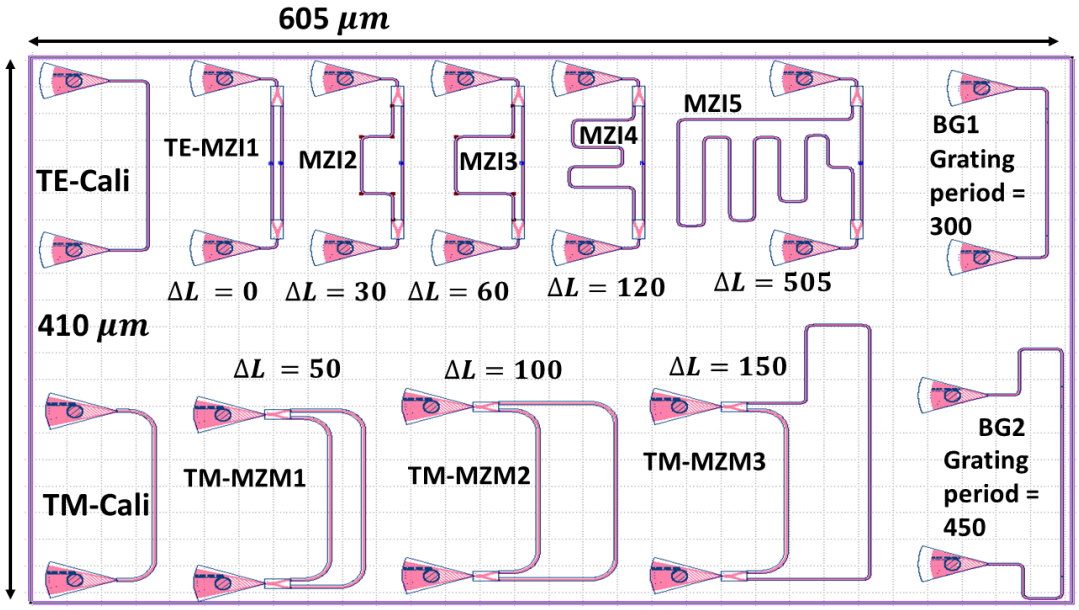

Fig. 15: Final version of the designed devices.

licon carrier wafer using perfluoropolyether vacuum oil.

5.2 Applied Nanotools, Inc. NanoSOI process:

The photonic devices were fabricated using the NanoSOI MPW fabrication process by Applied Nanotools Inc. (`http://www.appliednt.com/nanosoi`; Edmonton, Canada) which is based on direct-write 100 keV electron beam lithography technology. Silicon-on-insulator wafers of 200 mm diameter, 220 nm device thickness and 2 μm buffer oxide thickness are used as the base material for the fabrication. The wafer was pre-diced into square substrates with dimensions of 25x25 mm, and lines were scribed into the substrate backsides to facilitate easy separation into smaller chips once fabrication was complete. After an initial wafer clean using piranha solution (3:1 H2SO4:H2O2) for 15 minutes and water/IPA rinse, hydrogen silsesquioxane (HSQ) resist was spin-coated onto the substrate and heated to evaporate the solvent. The photonic devices were patterned using a Raith EBPG 5000+ electron beam instrument using a raster step size of 5 nm. The exposure dosage of the design was corrected for proximity effects that result from the backscatter of electrons from exposure of nearby features. Shape writing order was optimized for efficient patterning and minimal beam drift. After the e-beam exposure and subsequent development with a tetramethylammonium sulfate (TMAH) solution, the devices were inspected optically for residues and/or defects. The chips were then mounted on a 4" handle wafer and underwent an anisotropic ICP-RIE etch process using chlorine after qualification of the etch rate. The resist was removed from the surface of the devices using a 10:1 buffer oxide wet etch, and the devices were inspected using a scanning electron microscope (SEM) to verify patterning and etch quality. A 2.2 μm oxide cladding was deposited using a plasma-enhanced chemical vapour deposition (PECVD) process based on tetraethyl orthosilicate (TEOS) at 300^{o}C. Reflectrometry measurements were performed throughout the process to verify the device layer, buffer oxide and cladding thicknesses before delivery.

6 Experimental Data

To characterize the devices, a custom-built automated test setup [[3]] with automated control software written in Python was used (`http://siepic.ubc.ca/probestation`). An Agilent 81600B tunable laser was used as the input source and Agilent 81635A optical power sensors as the output detectors. The wavelength was swept from 1500 to 1600 nm in 10 pm steps. A polarization maintaining (PM) fibre was used to maintain the polarization state of the light, to couple the TE polarization into the grating couplers [[4]]. A 90^{o} rotation was used to inject light into the TM grating couplers [4]. A polarization maintaining fibre array was used to couple light in/out of the chip [www.plcconnections.com].

Plots of experimental data. The following figure was generated using a built-in Python interpreter!

7 Analysis

The free spectral range (FSR) of the MZI is related to the group index by

$$\mathrm{FSR} = \frac{\lambda^2}{n_g \Delta L}. \tag{10}$$

Rearranging, the group index can be extracted from measured data as

$$n_g = \frac{\lambda^2}{\mathrm{FSR} \cdot \Delta L}. \tag{11}$$

Using the simulated transmission spectra, the FSR is extracted by measuring the wavelength spacing between adjacent transmission maxima. The resulting group index shows excellent agreement with eigenmode simulation results. The same procedure will be applied to experimentally measured spectra following fabrication.

Rest will be updated in future after chip fabrication and getting experimental data for analysis

8 Conclusion

Rest will be updated in future after chip fabrication and getting experimental data for analysis

9 Acknowledgements

(edit according to your use).

I/We acknowledge the edX UBCx Phot1x Silicon Photonics Design, Fabrication and Data Analysis course, which is supported by the Natural Sciences and Engineering Research Council of Canada (NSERC) Silicon Electronic-Photonic Integrated Circuits (SiEPIC) Program. The devices were fabricated by Richard Bojko at the University of Washington Washington Nanofabrication Facility, part of the National Science Foundation's National Nanotechnology Infrastructure Network (NNIN), and Cameron Horvath at Applied Nanotools, Inc. Enxiao Luan performed the measurements at The University of British Columbia. We acknowledge Lumerical Solutions, Inc., Mathworks, Mentor Graphics, Python, and KLayout for the design software.

References

1. Chrostowski L, Hochberg M (2015) Silicon Photonics Design. Cambridge University Press (CUP)

2. Bojko RJ, Li J, He L, et al. (2011) Electron beam lithography writing strategies for low loss high confinement silicon optical waveguides. Journal of Vacuum Science & Technology B: Microelectronics and Nanometer Structures 29:06F309. https://doi.org/10.1116/1.3653266

3. Chrostowski L, Hochberg M Testing and packaging. In: Silicon Photonics Design. Cambridge University Press (CUP), pp 381–405

4. Wang Y, Wang X, Flueckiger J, et al. (2014) Focusing sub-wavelength grating couplers with low back reflections for rapid prototyping of silicon photonic circuits. Opt Express 22:20652. https://doi.org/10.1364/oe.22.020652